Available online at www.sciencedirect.com

ScienceDirect

IFAC PapersOnLine 56-2 (2023) 2226–2231

Enforcing Safety for Mixed Traffic Control via a Control Barrier Function Quadratic Program

Chenguang Zhao, Huan Yu *

The Hong Kong University of Science and Technology (Guangzhou), Thrust of Intelligent Transportation, Nansha, Guangzhou, 511400, Guangdong, China.

Abstract: Connected Automated Vehicle (CAV) has been considered as a transformative technology to improve traffic performance from various aspects. Many recent efforts have focused on the control of CAVs to dissipate stop-and-go waves in mixed-autonomy traffic. However, the safety impact of the CAV control design has not been fully addressed. A feedback controller that stabilizes the mixed vehicle platoon could cause rear-end collisions in some safety-critical scenarios, which hinders the application of CAV control design. This paper focuses on designing a Safety-critical Traffic Controller (STC) for a leading CAV that guarantees both safety and stability in the closed-loop mixed traffic system. We first propose the safe driving constraints for CAV and HDVs, based on which we design Control Barrier Functions (CBF) to penalize a nominal control input for any safety violation. We synthesize a safety-critical controller by integrating the CBF constraints with a nominal controller that achieves string stability and then solving a Quadratic Programming (QP) problem. Numerical simulations demonstrate that the proposed STC guarantees safety and expands the safety region of the mixed system. Simulations on the NGSIM dataset further validate that STC avoids rear-end collisions in real traffic.

Keywords: connected and automated vehicle, mixed traffic, string stability, safety-critical control, control barrier function

1. INTRODUCTION

Connected and Automated Vehicle (CAV) has received considerable attention due to its potential to improve traffic performance from multiple aspects, such as increasing traffic capacity (Chen et al., 2017), improving the stability of traffic flow (Talebpour and Mahmassani, 2016), and increasing road safety (Wang et al., 2020b; Ye and Yamamoto, 2019). Despite the promising benefits brought by CAVs, there will be an inevitable long transition period when the traffic is in mixed autonomy; namely, CAVs coexist with Human Driven Vehicles (HDVs). Therefore, control of CAVs in mixed autonomy traffic has been studied extensively over the past decade (Molnár et al., 2020; Stern et al., 2018).

One main role of the CAV controller is to enhance traffic flow stability and to dissipate the so-called stop-and-go waves, which cause alternating acceleration and deceleration of vehicles. In (Cui et al., 2017), the authors propose that one single autonomous vehicle can locally stabilize traffic flow in a ring road setting. It is demonstrated by a field experiment in (Stern et al., 2018) that feedback control of a leading autonomous vehicle can dampen stop-and-go waves in the following HDVs. The stabilization of mixed traffic with multiple CAVs is further studied in (Wang et al., 2020a, 2022b; Zheng et al., 2020), which focused on achieving head-to-tail string stability of mixed autonomy through different types of feedback information topology enabled by Vehicle-to-Vehicle communication and coordination of actuation by automated vehicles (Darbha et al., 2018). To exploit CAV's potential, multiple control strategies have been proposed to stabilize mixed traffic. The Adaptive Cruise Control (ACC) (Kesting et al., 2008) and cooperative Adaptive Cruise Control (CACC) (Dey et al., 2015) control the CAV by input states from head vehicles, and the Connected Cruise Control (CCC) observes the following vehicles' states to control the CAV (Orosz, 2016). In (Wang et al., 2022a), the notion of Leading Cruise Control (LCC) is proposed, where a feedback controller for the CAV is designed with input states from both leading and following vehicles.

Beyond the scope of stability, traffic safety evaluation is of vital importance before considering the adoption of any stabilizing CAV control strategies in the traffic system. Although many studies have discussed the potential influence of CAVs on traffic safety given the ratio of CAVs in mixed traffic (Arvin et al., 2020; Rahman and Abdel-Aty, 2018; Ye and Yamamoto, 2019), the research on whether the controller of a CAV can guarantee mixed traffic safety, especially in critical conditions, is still insufficient. It is shown in (Dai et al., 2022) that a CAV controller that achieves string stability may cause unsafe rear-end collisions in a controlled platoon. Therefore, both safety and stability need to be considered jointly for the CAV control in mixed traffic, which has not been addressed to the best knowledge of authors. When there are potential conflicts between safety and stability in some safety-critical scenarios, stability needs to be sacrificed to give priority for maintaining safety. In particular, we propose a safe control framework that synthesizes a feed-

⋆ Corresponding author, email: huanyu@ust.hk

10.1016/j.ifacol.2023.10.1151

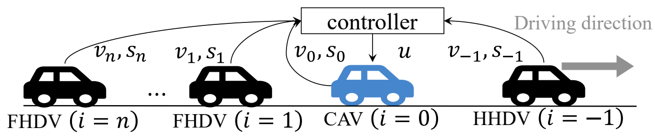

Fig. 1. We consider the control for a CAV following a Head HDV and leading n Following HDVs. Given a nominal controller that achieves string stability for the mixed platoon, the proposed safety-critical traffic controller synthesizes a safe control input to maintain safe spacing for all vehicles in the controlled system.

back controller with a user-chosen nominal controller and a Control Barrier Function Quadratic Program (CBF-QP) redesign (Ames et al., 2019; Krstic, 2021), simultaneously achieving safety and stability for the mixed system. The CBF has been adopted in multiple areas, such as multi-robot systems (Chen et al., 2020), and quadrotors (Xu and Sreenath, 2018). In this paper, we utilize CBF to guarantee safety for mixed autonomy. Previous work of the author (Zhou and Yu, 2022) integrates CBF into car-following traffic control to maintain the safety of mixed autonomy. In this paper, we further extend the previous work by designing a safety-critical controller with less computation cost and testing it with real traffic data.

In this paper, we aim to design a safety-critical CAV controller that avoids rear-end collision for its own safety consideration and for the following HDVs as well. We design and validate the safety-critical controller from the following aspects:

- We define a safe longitudinal car-following policy for both the leading CAV and the following HDVs to guarantee collision-free safety of the mixed traffic system. To achieve the safe driving requirement, we employ Control Barrier Function (CBF) (Ames et al., 2019; Krstic, 2021) to impart safety on the controlled system. In particular, we design CBF candidates with the relative degree one for both the CAV and HDVs, which reduces the computation complexity and cost compared with high-order CBF (Zhou and Yu, 2022).
- We propose a Safety-critical Traffic Control (STC) framework, which provides safety guarantee for a nominal controller that is pre-designed to stabilize the traffic for head-to-tail string stability. The safety constraints defined by CBF restrict the nominal control input and deviate it from violation when necessary. The conflict between safety and stability is mediated at a minimum cost by solving a Quadratic Programming (QP) problem.
- We specify a risky scenario where the head vehicle suddenly decelerates to demonstrate the safety improvement of the STC controller. We delineate and compare the maximum safe duration of HHDV's deceleration of the nominal controller and the designed STC controller. We further validate the STC controller on the Next Generation Simulation (NGSIM) dataset. Results show that while the nominal controller causes rear-end collision, the STC controller guarantees safety for the mixed autonomy.

2. MICROSCOPIC TRAFFIC MODEL FOR MIXED AUTONOMY

In this section, we first introduce the microscopic traffic model that describes the acceleration of a vehicle given the traffic states, i.e., speed and gap. Then we linearize the model and derive the mixed autonomy traffic model.

2.1 Car-following model for HDVs and CAV

We consider a platoon of n HDVs led by a CAV. The CAV follows a Head HDV (HHDV) and leads n Following HDVs (FHDVs), as shown in Fig. 1.

We use a microscopic model to describe the car-following motions of FHDVs. For a vehicle i, the dynamics of its microscopic states, gap s_i and velocity v_i, are given by

$$\dot{s}_i(t) = v_{i-1}(t) - v_i(t), \tag{1}$$
$$\dot{v}_i(t) = F\left(s_i(t), \dot{s}_i(t), v_i(t)\right), \tag{2}$$

where v_{i-1} is its leader's speed, F is an acceleration function describing the driver's driving strategy dependent on its speed v_i and gap s_i. One straightforward and widely-adopted functional form is the Full Velocity Difference Model (FVDM), which gives the acceleration as

$$\dot{v}_i = \alpha(V(s_i) - v_i) + \beta \dot{s}_i, \tag{3}$$

where $V(s)$ is the desired speed-gap relationship. We take the $V(s)$ adopted in (Wang et al., 2022a; Zheng et al., 2020) as:

$$V(s) = \begin{cases} 0, & s \le s_{\mathrm{st}}, \\ \frac{v_{\max}}{2}\left(1 - \cos\left(\pi \frac{s - s_{\mathrm{st}}}{s_{\mathrm{go}} - s_{\mathrm{st}}}\right)\right), & s_{\mathrm{st}} < s < s_{\mathrm{go}}, \\ v_{\max}, & s \ge s_{\mathrm{go}}. \end{cases} \tag{4}$$

Based on the gap between vehicles, the desired speed is divided into three formulations:

- When the gap is smaller than the low-threshold s_{st}, the desired speed is zero, which means the gap is unsafe and the vehicle should stop.
- When the gap is larger than the up-threshold s_{go}, the leader vehicle is too far to influence drivers' decision, and the vehicle cruises at the maximum speed $v_{\max}$.
- When the gap is between the two thresholds, the driver is in the car-following model, and cruises considering both its state and the leader vehicle's state.

For the CAV, its gap is determined by its speed $v_0(t)$ and the speed of its leader HHDV. The CAV's longitudinal acceleration is directly actuated by the control input $u(t)$, and we have the CAV car-following model as

$$\dot{s}_0(t) = v_{-1}(t) - v_0(t), \tag{5}$$
$$\dot{v}_0(t) = u(t), \tag{6}$$

with $v_{-1}(t)$ being the HHDV's speed.

2.2 Steady states and linearized model

As linear string stability of the mixed system will be discussed, we first linearize the FVDM model (3) around an equilibrium speed v^* and the corresponding equilibrium gap $s^* = V(s^*)$. The small deviation of states from the equilibrium states (v^*, s^*) is defined as

$$\tilde{s}_i(t) = s_i(t) - s^*, \tag{7}$$
$$\tilde{v}_i(t) = v_i(t) - v^*, \tag{8}$$

for the CAV with $i=0$ and FHDVs with $i=1,2,\cdots,n$. The FVDM (3) is then linearized as

$$\dot{\tilde{s}}_i(t)=\tilde{v}_{i-1}(t)-\tilde{v}_i(t), \tag{9}$$

$$\dot{\tilde{v}}_i(t)=\alpha_1\tilde{s}_i(t)-\alpha_2\tilde{v}_i(t)+\alpha_3\tilde{v}_{i-1}(t), \tag{10}$$

where the parameters are

$$\alpha_1=\frac{\partial F}{\partial s}=\alpha\left.\frac{\mathrm{d}V}{\mathrm{d}s}\right|_{s=s^*}, \tag{11}$$

$$\alpha_2=\frac{\partial F}{\partial \dot{s}}-\frac{\partial F}{\partial v}=\alpha+\beta, \tag{12}$$

$$\alpha_3=\frac{\partial F}{\partial \dot{s}}=\beta. \tag{13}$$

To make the model physically practical, the coefficients should satisfy $\alpha_1>0$, $\alpha_2>0$, and $\alpha_3>0$, which means the vehicle will accelerate when: 1) its gap increases; 2) its speed decreases; or 3) the leader accelerates. Such a driving strategy is consistent with most human driving behaviors.

Considering the mixed CAV-HDV platoon, we define the state variable for the platoon as

$$x=[\tilde{s}_0,\tilde{v}_0,\tilde{s}_1,\tilde{v}_1,\cdots,\tilde{s}_n,\tilde{v}_n]^{\mathrm{T}}\in\mathbb{R}^{2n+2}, \tag{14}$$

and the dynamics of the platoon are

$$\dot{x}(t)=Ax(t)+Bu(t)+D\tilde{v}_{-1}(t), \tag{15}$$

where the system matrix is

$$A=\begin{bmatrix}P_0 & & & \\ P_2 & P_1 & & \\ & \ddots & \ddots & \\ & & P_2 & P_1\end{bmatrix}\in\mathbb{R}^{(2n+2)\times(2n+2)}, \tag{16}$$

with

$$P_0=\begin{bmatrix}0 & -1\\ 0 & 0\end{bmatrix},\ P_1=\begin{bmatrix}0 & -1\\ \alpha_1 & -\alpha_2\end{bmatrix},\ P_2=\begin{bmatrix}0 & 1\\ 0 & \alpha_3\end{bmatrix}, \tag{17}$$

and the input vector is

$$B=[0,1,0,0,\cdots,0]^{\mathrm{T}}\in\mathbb{R}^{2n+2}, \tag{18}$$

and the speed variation of the HHDV $\tilde{v}_{-1}$ is regarded as the input disturbance with

$$D=[1,0,0,0,\cdots,0]^{\mathrm{T}}\in\mathbb{R}^{2n+2}. \tag{19}$$

3. SAFETY-CRITICAL TRAFFIC CONTROL VIA CBF-QP

In this section, we first give a nominal controller that achieves string stability but without safety guarantee for the mixed platoon. Then we introduce the safe driving policy for the CAV and HDVs, based on which we design a CBF-QP to achieve safety-critical stabilization.

3.1 State-feedback nominal controller for string stability

String stability refers to the property that a perturbation of the leader vehicle's state will be dampened out by the follower vehicles. For a platoon, the head-to-tail string stability is more widely adopted, with the definition as follows.

Definition 1. (Head-to-tail string stability). (Jin and Orosz, 2014) For a platoon, it is head-to-tail string stable if and only if

$$\forall\omega>0,\quad |\Gamma(j\omega)|^2<1, \tag{20}$$

where $j^2=-1$, and the head-to-tail transfer function Γ is defined as

$$\Gamma(s)=\frac{\tilde{V}_{\mathrm{t}}(s)}{\tilde{V}_{\mathrm{h}}(s)}, \tag{21}$$

with $\tilde{V}_{\mathrm{t}}$ and $\tilde{V}_{\mathrm{h}}$ being the Laplace transform of the tail and head vehicle's speed deviation $\tilde{v}_{\mathrm{t}}$ and $\tilde{v}_{\mathrm{h}}$ respectively.

To achieve head-to-tail string stability of the platoon, a state-feedback controller for the CAV is proposed in (Wang et al., 2022a) as:

$$u_0=\alpha_1\tilde{s}_0-\alpha_2\tilde{v}_0+\alpha_3\tilde{v}_{-1}+\sum_{i=1}^{n}(\mu_i\tilde{s}_i+k_i\tilde{v}_i), \tag{22}$$

where μ_i is the feedback gain for FHDV i's gap, and k_i is the feedback gain for FHDV i's speed. The transfer function $\Gamma(s)$ given the controller (22) can be referred to (Wang et al., 2022a).

With proper choice of feedback gains μ_i,k_i, the controller (22) achieves string stability, i.e., perturbation from the HHDV will not cause severe stop-and-go acceleration and deceleration of the FHDVs in the closed-loop system. However, the controller (22) does not consider traffic safety, which in the following content, we refer to (22) as a nominal controller and redesign it to achieve safety-critical traffic control. It should be noted that the STC design and the safety framework can be generalized to other choices of nominal controllers.

3.2 Safety-critical traffic control via CBF

In this subsection, we combine the pre-designed nominal controller (22) and CBF to achieve safe driving. We first give the safe driving policy for CAV and HHDVs, then we introduce CBF candidates and design a CBF-QP for safety-critical control.

Safe driving constraints To avoid possible collisions with the leading vehicle, a vehicle should keep a safe gap in driving. We define the safe driving policy for the vehicle i as

$$s_i\geq\tau v_i, \tag{23}$$

where $\tau>0$ is a safe time headway. For the CAV with $i=0$, the policy (23) requires that it should keep a safe gap with the HHDV to avoid an accident in case of sudden deceleration of HHDV, which might happen due to a risky cut-in lane-changing vehicle. For the FHDV $i=1,\cdots,n$, it should keep a safe safe gap with its leader in case of some sudden acceleration caused by fatigue or aggressive driving of the follower driver.

Based on the safe driving policy (23), we define the safe set for vehicle i as

$$\mathcal{C}_i=\{x|\tilde{s}_i+s^*\geq\tau\left(\tilde{v}_i+v^*\right)\}. \tag{24}$$

For the vehicle i, if its initial state is in the safe set, i.e, $s_i(0)\geq\tau v_i(0)$, and it stays in the safe set with $x(t)\in\mathcal{C}_i$ $\forall t>0$, then we call the safe set $\mathcal{C}_i$ to be forward invariant.

A safety-critical controller should make the safe set forward invariant to avoid accidents. To design such a controller, we adopt the control barrier function, since its property of generating forward invariant safe set (Ames et al., 2019).

Definition 2. (Control barrier function). (Ames et al., 2019) For an affine control system

$$\dot{x} = f(x) + g(x)u, \tag{25}$$

with $x \in \mathbb{R}^{n_1}$, $u \in \mathbb{R}^{n_2}$, a continuously differentiable function $h : \mathbb{R}^{n_1} \to \mathbb{R}$ is a control barrier function for the system if there exists an extended $\mathcal{K}_\infty$ function $\gamma : \mathbb{R} \to \mathbb{R}$ such that

$$\forall x \in \mathbb{R}, \quad \sup_u [L_f h(x) + L_g h(x)u] \geq -\gamma(h(x)), \tag{26}$$

where $L_f h = \nabla h(x) \cdot f(x)$ and $L_g h = \nabla h(x) \cdot g(x)$ are the Lie derivatives.

For a continusoutly differentiable function $h : \mathbb{R}^{n_1} \to \mathbb{R}$, we define its safe set $\mathcal{C} \subset \mathbb{R}^{n_1}$ as the 0-superlevel set of h:

$$\mathcal{C} = \{x \in \mathbb{R}^{n_1} | h(x) \geq 0\}. \tag{27}$$

We have the following theorem stating the property of CBF that it renders forward invariant safe set $\mathcal{C}$:

Theorem 1. (Ames et al., 2019) If $h(x)$ is a control barrier function for the system (25), then any Lipschitz controller $u(x)$ that satisfies

$$L_f h(x) + L_g h(x)u \geq -\gamma(h(x)), \tag{28}$$

renders the safe set $\mathcal{C}$ defined in (27) forward invariant.

Comparing (25) and the mixed-autonomy traffic model (14), we can see that $f(x) = Ax + D\tilde{v}_{-1}$ and $g(x) = B$. Based on the safe driving policy (23), we design the CBF candidate for the CAV as

$$h_0(x) = s_0 - \tau v_0 = \tilde{s}_0 + \tau\tilde{v}_0 + s^* - \tau v^*. \tag{29}$$

For FHDV i, the CBF candidate directly derived from the safe driving policy (23) is

$$h_i(x) = s_i - \tau v_i = \tilde{s}_i + \tau\tilde{v}_i + s^* - \tau v^*. \tag{30}$$

For $h_i(x)$, we can check that its relative degree to the CAV control input is $i+1$. Although we can introduce high relative order CBF, a CBF candidate with a relative degree higher than one will complicate the system output solution and make it sensitive to parameters (Ames et al., 2019). Therefore, we further introduce the reduced-degree CBF candidate for FHDVs as

$$\begin{aligned} h_i^{\mathrm{r}}(x) &= h_i(x) - h_0(x) = s_i - s_0 - \tau(v_i - v_0) \\ &= \tilde{s}_i - \tilde{s}_0 - \tau\left(\tilde{v}_i - \tilde{v}_0\right). \end{aligned} \tag{31}$$

It is easy to check that the above reduced-degree candidates $h_i^{\mathrm{r}}(x)$ in (31) have a relative degree one. We also note that when $h_0(x) \geq 0$ and $h_i^{\mathrm{r}}(x) \geq 0$, the original $h_i(x)$ is also non-negative, which means the safe driving constraint for FHDVs is satisfied.

Combing the nominal controller u_0 in (22) and the CBF candidates in (29), (31), we introduce the following CBF-QP problem,

$$\underset{u \in \mathbb{R}}{\arg\min} \; |u - u_0|^2 \tag{32}$$

$$\text{s.t.} \; L_f h_0(x) + L_g h_0(x)u + \gamma(h_0(x)) \geq 0, \tag{33}$$

$$L_f h_i^{\mathrm{r}}(x) + L_g h_i^{\mathrm{r}}(x)u + \gamma(h_i^{\mathrm{r}}(x)) \geq 0, \quad \forall i = 1, 2, \cdots, n, \tag{34}$$

$$a_{\min} \leq u \leq a_{\max}, \tag{35}$$

The safety constraint for CAV in (33) guarantees that CAV will keep a safe gap with HHDV, and the safety constraint for FHDVs is in (34). The constraint (35) restricts the acceleration of CAV between the minimum acceleration $a_{\min}$ and maximum acceleration $a_{\max}$ to avoid uncomfortable or physically unrealistic acceleration.

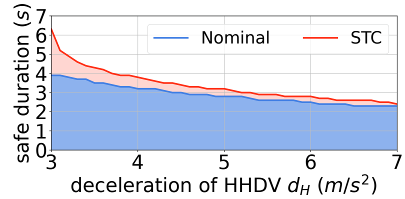

Fig. 2. Safety region of the nominal controller and the proposed STC controller.

From the formulated QP problem (32), we can see that when the nominal controller u_0 (22) that is designed to stabilize traffic gives safe acceleration, we will use it to control the CAV. But when the nominal controller renders an unsafe driving strategy, the CBF is activated, and the proposed STC will guarantee the safe policy is met.

4. SIMULATION

In this section, we run numerical simulations to test the proposed STC controller. We first give the simulation setting, and then we compare the performance of the nominal controller and the STC controller. We also provide an analysis of the control output of the proposed STC controller and how it improves safety over the nominal controller.

4.1 Experiment Setting

In the simulation, we consider the platoon of one CAV and $n = 2$ FHDVs. For the microscopic model FVDM (3), we set $\alpha = 0.6$, $\beta = 0.9$. For the desired gap-velocity relationship $V(s)$ in (4), we set the threshold for stop as $s_{\mathrm{st}} = 5$ m, the threshold for free driving as $s_{\mathrm{go}} = 35$ m, and the maximum speed as $v_{\max} = 40$ m/s. We assume that initially at $t = 0$, the platoon drivers at the equilibrium speed $v^* = 20$ m/s, and each vehicle keeps a each equilibrium gap $s^* = 20$ m.

We consider one risky scenario that may happen in practice: the sudden deceleration of HHDV. When there is a dangerous cutting-in lane-changing or a jaywalking pedestrian, the HHDV's driver will take an emergency brake to avoid a crash. We suppose that the HHDV starts to decelerate at 5 s with a deceleration of d_H, and the braking of the HHDV lasts for a duration of t_H. After $5+t_H$, we let the HHDV accelerates with an acceleration of $-d_H$ and a duration of t_H, which means the HHDV will recover to the equilibrium speed v^* after $5+2t_H$. The CAV is controlled by the nominal controller (22) or the STC controller (32). The two FHDVs adjust their acceleration based on the microscopic model in (3).

For the nominal controller in (22), we set the feedback gains as $\mu_1 = -2$, $k_1 = 0.2$, $\mu_2 = -2$, and $k_2 = 0.2$. For the extended $\mathcal{K}_\infty$ function in (33) and (34), we take it as $\gamma(x) = 10x$. We take the safe headway in (23) as $\tau = 0.4$ s. We set the minimum and maximum acceleration in (35) as $a_{\min} = -7$ m/s^2 and $a_{\max} = 7$ m/s^2 respectively.

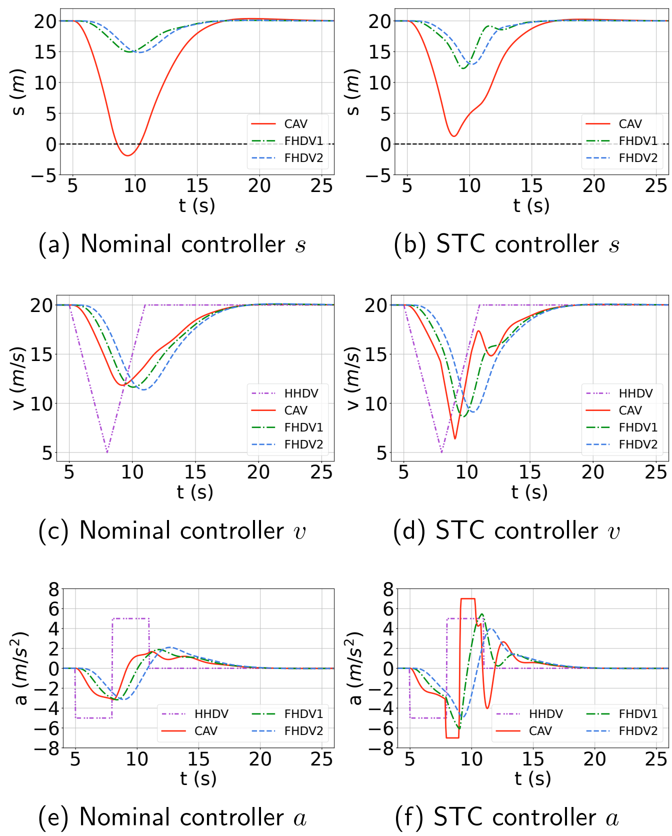

(a) Nominal controller s (b) STC controller s

(c) Nominal controller v (d) STC controller v

(e) Nominal controller a (f) STC controller a

Fig. 3. Profile of gap, speed, and acceleration under the nominal controller and STC controller.

4.2 Comparison with nominal controller

We first compare the safety region for the nominal controller and the proposed STC controller. We vary the deceleration of the HHDV d_H from 3 m/s^2 to 7 m/s^2, and give the safe range of duration of deceleration t_H under which there is no rear-end collision in the platoon. The result is given in Fig. 2. The blue-shaded region is the safety region of the nominal controller, and the red-shaded area is the expanded safety region brought by the proposed STC controller. We see that the proposed STC controller has a larger safety region than the nominal controller, which demonstrates the improvement in safety brought by the designed STC controller.

To further analyze the performance of the proposed STC controller, we plot and compare the profile of gap s_i, speed v_i, and acceleration a_i generated under the two controllers in Fig.3 with $d_H = 5$ m/s^2 and $t_H = 3$ s. From Fig.3(e) and (f), it can be seen that after 5 s when the HHDV begins to decelerate, the STC controller yield a larger deceleration of CAV, which also makes the FHDVs brakes more sharply. Such a larger deceleration brings the lower speed of the CAV and FHDVs, as shown in Fig.3(c) and (d), which increases the gap between CAV and the HHDV and avoids collision as in Fig.3(a) and (b).

4.3 Validation on the NGSIM dataset

In this section, we validate the proposed STC controller on the NGSIM dataset.

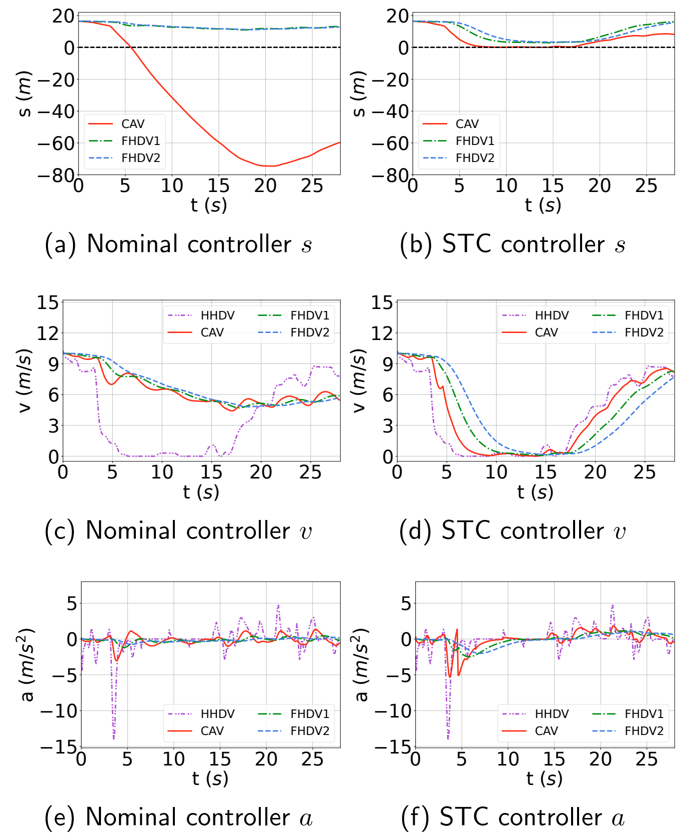

(a) Nominal controller s (b) STC controller s

(c) Nominal controller v (d) STC controller v

(e) Nominal controller a (f) STC controller a

Fig. 4. Profile of gap, speed, and acceleration under the nominal controller and STC controller on the NGSIM dataset.

The NGSIM dataset records trajectory data of vehicles at Emeryville, California with a resolution of 0.1 s. We use the trajectory reconstructed by (Montanino and Punzo, 2015), which has removed some measurement errors or physically unreasonable driving behavior. We calibrate the model parameters for the FVDM (3) as $\alpha = 0.16$, $\beta = 0.63$, $s_{\mathrm{st}} = 1.6$ m, $s_{\mathrm{go}} = 50$ m, and $v_{\max} = 46.9$ m/s by trajectories in the dataset.

We identify Vehicle-2169 from the dataset, which has an emergency brake as shown by the purple line in Fig. 4(e). We take its speed and acceleration profiles as those for the HHDV to test whether there will be collisions in the mixed autonomy. For the equilibrium states, we take the equilibrium speed v^* as the initial speed of Vehicle-2169 in the dataset and get the equilibrium speed s^* by $F(s^*, 0, v^*) = 0$. We set the initial speed of CAV and two FHDVs as v^* and their initial gap as s^*, i.e., $v_0(0) = v_1(0) = v_2(0) = v^*$, $s_0(0) = s_1(0) = s_2(0) = s^*$. For the nominal controller (22), we take the feedback gain as $\mu_1 = \mu_2 = -2$ and $k_1 = k_2 = 0.2$, which satisfies the string stability condition (20). For the STC, we take the safe time headway (23) as $\tau = 1$ s and the extended $\mathcal{K}_\infty$ function as $r(x) = 10x$.

In Fig. 4, we plot the gap s, speed v, and acceleration a of the platoon got by the nominal controller and the STC controller. We see that the nominal controller causes a collision, but the STC controller ensures the safety of the mixed autonomy platoon.

5. CONCLUSION

In this paper, we studied the safety-critical control of mixed traffic by a leading CAV. We proposed a safe driving policy for CAV and HDVs and accordingly designed CBF candidates for both types of vehicles. An STC controller has been proposed, which combines a pre-designed nominal controller with string stability and CBF constraints via QP to simultaneously guarantee the safety and stability of mixed traffic. We analyzed the safety region of the STC controller and demonstrated that safety is enhanced by relaxing stability conditions for smoothing the mixed traffic. The safety improvement was further validated on the NGSIM dataset. Future work of interest lies in developing safe-critical coordination control of multiple CAVs for mixed traffic, as well as exploring alternative safe driving policies.

REFERENCES

Ames, A.D., Coogan, S., Egerstedt, M., Notomista, G., Sreenath, K., and Tabuada, P. (2019). Control barrier functions: Theory and applications. In *2019 18th European control conference (ECC)*, 3420–3431. IEEE.

Arvin, R., Khattak, A.J., Kamrani, M., and Rio-Torres, J. (2020). Safety evaluation of connected and automated vehicles in mixed traffic with conventional vehicles at intersections. *Journal of Intelligent Transportation Systems*, 25(2), 170–187.

Chen, D., Ahn, S., Chitturi, M., and Noyce, D.A. (2017). Towards vehicle automation: Roadway capacity formulation for traffic mixed with regular and automated vehicles. *Transportation research part B: methodological*, 100, 196–221.

Chen, Y., Singletary, A., and Ames, A.D. (2020). Guaranteed obstacle avoidance for multi-robot operations with limited actuation: A control barrier function approach. *IEEE Control Systems Letters*, 5(1), 127–132.

Cui, S., Seibold, B., Stern, R., and Work, D.B. (2017). Stabilizing traffic flow via a single autonomous vehicle: Possibilities and limitations. In *2017 IEEE Intelligent Vehicles Symposium (IV)*, 1336–1341. IEEE.

Dai, Y., Yang, Y., Wang, Z., and Luo, Y. (2022). Exploring the impact of damping on connected and autonomous vehicle platoon safety with cacc. *Physica A: Statistical Mechanics and its Applications*, 128181.

Darbha, S., Konduri, S., and Pagilla, P.R. (2018). Benefits of v2v communication for autonomous and connected vehicles. *IEEE Transactions on Intelligent Transportation Systems*, 20(5), 1954–1963.

Dey, K.C., Yan, L., Wang, X., Wang, Y., Shen, H., Chowdhury, M., Yu, L., Qiu, C., and Soundararaj, V. (2015). A review of communication, driver characteristics, and controls aspects of cooperative adaptive cruise control (cacc). *IEEE Transactions on Intelligent Transportation Systems*, 17(2), 491–509.

Jin, I.G. and Orosz, G. (2014). Dynamics of connected vehicle systems with delayed acceleration feedback. *Transportation Research Part C: Emerging Technologies*, 46, 46–64.

Kesting, A., Treiber, M., Schönhof, M., and Helbing, D. (2008). Adaptive cruise control design for active congestion avoidance. *Transportation Research Part C: Emerging Technologies*, 16(6), 668–683.

Krstic, M. (2021). Inverse optimal safety filters. *arXiv preprint arXiv:2112.08225*. Unpublished.

Molnár, T.G., Upadhyay, D., Hopka, M., Van Nieuwstadt, M., and Orosz, G. (2020). Open and closed loop traffic control by connected automated vehicles. In *2020 59th IEEE Conference on Decision and Control (CDC)*, 239–244. IEEE.

Montanino, M. and Punzo, V. (2015). Trajectory data reconstruction and simulation-based validation against macroscopic traffic patterns. *Transportation Research Part B: Methodological*, 80, 82–106.

Orosz, G. (2016). Connected cruise control: modelling, delay effects, and nonlinear behaviour. *Vehicle System Dynamics*, 54(8), 1147–1176.

Rahman, M.S. and Abdel-Aty, M. (2018). Longitudinal safety evaluation of connected vehicles' platooning on expressways. *Accident Analysis & Prevention*, 117, 381–391.

Stern, R.E., Cui, S., Delle Monache, M.L., Bhadani, R., Bunting, M., Churchill, M., Hamilton, N., Pohlmann, H., Wu, F., Piccoli, B., et al. (2018). Dissipation of stop-and-go waves via control of autonomous vehicles: Field experiments. *Transportation Research Part C: Emerging Technologies*, 89, 205–221.

Talebpour, A. and Mahmassani, H.S. (2016). Influence of connected and autonomous vehicles on traffic flow stability and throughput. *Transportation Research Part C: Emerging Technologies*, 71, 143–163.

Wang, J., Zheng, Y., Chen, C., Xu, Q., and Li, K. (2022a). Leading cruise control in mixed traffic flow: System modeling, controllability, and string stability. *IEEE Transactions on Intelligent Transportation Systems*, 23(8), 12861–12876.

Wang, J., Zheng, Y., Xu, Q., Wang, J., and Li, K. (2020a). Controllability analysis and optimal control of mixed traffic flow with human-driven and autonomous vehicles. *IEEE Transactions on Intelligent Transportation Systems*, 22(12), 7445–7459.

Wang, L., Zhong, H., Ma, W., Abdel-Aty, M., and Park, J. (2020b). How many crashes can connected vehicle and automated vehicle technologies prevent: a meta-analysis. *Accident Analysis & Prevention*, 136, 105299.

Wang, S., Shang, M., Levin, M.W., and Stern, R. (2022b). Smoothing nonlinear mixed traffic with autonomous vehicles: Control design. In *2022 IEEE 25th International Conference on Intelligent Transportation Systems (ITSC)*, 661–666. IEEE.

Xu, B. and Sreenath, K. (2018). Safe teleoperation of dynamic uavs through control barrier functions. In *2018 IEEE International Conference on Robotics and Automation (ICRA)*, 7848–7855. IEEE.

Ye, L. and Yamamoto, T. (2019). Evaluating the impact of connected and autonomous vehicles on traffic safety. *Physica A: Statistical Mechanics and its Applications*, 526, 121009.

Zheng, Y., Wang, J., and Li, K. (2020). Smoothing traffic flow via control of autonomous vehicles. *IEEE Internet of Things Journal*, 7(5), 3882–3896.

Zhou, J. and Yu, H. (2022). Safety critical control of mixed-autonomy traffic via a single autonomous vehicle. In *2022 IEEE 25th International Conference on Intelligent Transportation Systems (ITSC)*, 3089–3094. IEEE.